

Chapter 25

Calcium Channels and Calcium-Regulated Channels in Human Red Blood Cells



Lars Kaestner, Anna Bogdanova, and Stephane Egee

Abstract Free Calcium (Ca^{2+}) is an important and universal signalling entity in all cells, red blood cells included. Although mature mammalian red blood cells are believed to not contain organelles as Ca^{2+} stores such as the endoplasmic reticulum or mitochondria, a 20,000-fold gradient based on a intracellular Ca^{2+} concentration of approximately 60 nM vs. an extracellular concentration of 1.2 mM makes Ca^{2+} -permeable channels a major signalling tool of red blood cells. However, the internal Ca^{2+} concentration is tightly controlled, regulated and maintained primarily by the Ca^{2+} pumps PMCA1 and PMCA4. Within the last two decades it became evident that an increased intracellular Ca^{2+} is associated with red blood cell clearance in the spleen and promotes red blood cell aggregability and clot formation. In contrast to this rather uncontrolled deadly Ca^{2+} signals only recently it became evident, that a temporal increase in intracellular Ca^{2+} can also have positive effects such as the modulation of the red blood cells O_2 binding properties or even be vital for brief transient cellular volume adaptation when passing constrictions like small capillaries or slits in the spleen. Here we give an overview of Ca^{2+} channels and Ca^{2+} -regulated channels in red blood cells, namely the Gárdos channel, the non-selective voltage dependent cation channel, Piezo1, the NMDA receptor, VDAC, TRPC channels, $\text{Ca}_v2.1$, a Ca^{2+} -inhibited channel novel to red blood cells and i.a. relate these channels to the molecular unknown sickle cell disease conductance P_{sickle} . Particular attention is given to correlation of functional measurements with

L. Kaestner (✉)

Theoretical Medicine and Biosciences, Saarland University, Homburg, Germany

Experimental Physics, Saarland University, Saarbrücken, Germany

e-mail: lars_kaestner@me.com

A. Bogdanova

Red Blood Cell Research Group, Institute of Veterinary Physiology, Vetsuisse Faculty and the Zürich Center for Integrative Human Physiology (ZIHP), University of Zürich, Zürich, Switzerland

S. Egee

CNRS, UMR8227 LBI2M, Sorbonne Université, Roscoff, France

Laboratoire d'Excellence GR-Ex, Paris, France

© Springer Nature Switzerland AG 2020

M. S. Islam (ed.), *Calcium Signaling*, Advances in Experimental Medicine and Biology 1131, https://doi.org/10.1007/978-3-030-12457-1_25

625

molecular entities as well as the physiological and pathophysiological function of these channels. This view is in constant progress and in particular the understanding of the interaction of several ion channels in a physiological context just started. This includes on the one hand channelopathies, where a mutation of the ion channel is the direct cause of the disease, like Hereditary Xerocytosis and the Gárdos Channelopathy. On the other hand it applies to red blood cell related diseases where an altered channel activity is a secondary effect like in sickle cell disease or thalassemia. Also these secondary effects should receive medical and pharmacologic attention because they can be crucial when it comes to the life-threatening symptoms of the disease.

Keywords Gárdos channel · Non-selective voltage dependent cation channel · Piezo1 · NMDA receptor · VDAC · TRPC channel · Ca_v2.1 · Calcium-inhibited channel · P_{sickle} · Anaemia

25.1 Introduction to Calcium in Red Blood Cells

Free Calcium (Ca²⁺) is an important and universal second messenger in all cells [1, 2], red blood cells (RBCs) included [3–5]. This results in the abundance of Ca²⁺-binding proteins in RBCs with differing Ca²⁺ sensitivities as outlined in Fig. 25.1. Mature mammalian RBCs are believed to not contain organelles as Ca²⁺ stores such as the endoplasmic reticulum or mitochondria [6]. Compared to other cell types, where the Ca²⁺ liberated from stores within intracellular organelles can be used in the regulation of free cytosolic Ca²⁺ concentration and thereby Ca²⁺ signalling, in mammalian erythrocytes the control of free intracellular Ca²⁺ concentration must be done by regulation of membrane transport. A 20,000-fold gradient based on an intracellular Ca²⁺ concentration of approximately 60 nM vs. an extracellular concentration of 1.2 mM makes Ca²⁺-permeable channels a major signalling tool of RBCs. As historically RBCs served as the model cell to investigate membrane transport, it is well known that the internal Ca²⁺ concentration is tightly controlled, regulated and maintained primarily by the Ca²⁺ pumps PMCA1 and PMCA4 [4, 7]. The Ca²⁺ pumping in turn is regulated by multiple factors, such as the Ca²⁺ concentration itself [8], calmodulin [9], calpain [10], phospholipids and various kinases [11] or even self-association [12]. Within the last two decades it became evident that an increased intracellular Ca²⁺ is associated with RBC clearance in the spleen and promotes RBCs aggregability and clot formation [3, 13–16]. There was a long debate within the community whether this process should be called eryptosis [17], which is no longer recommended [18]. In contrast to this rather uncontrolled deadly Ca²⁺ signals (resulting in Ca²⁺ overload), within the recent years it became evident that a temporal increase in intracellular Ca²⁺ can also have positive effects such as the modulation of the RBCs O₂ binding properties [19] or even be vital for brief transient cellular volume adaptation when passing constrictions like small capillaries or slits in the spleen [5, 20, 21] as depicted in Fig. 25.2. The perilous balance of Ca²⁺ in RBCs was recently reviewed [3].

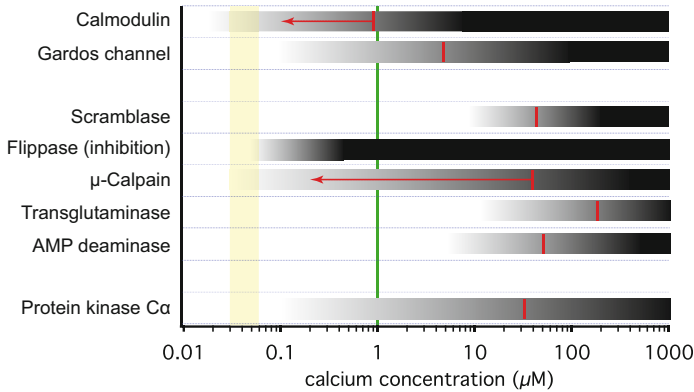


Fig. 25.1 Overview of concentration dependence of Ca^{2+} activated proteins in RBCs. The yellow column indicates the estimated range of RBCs' resting free Ca^{2+} [96]. The gray/black bars indicate the activation of the proteins with the intensity of darkness related to the activation level (details see below). The red lines depict the half activation concentration. For orientation the green line provides the in vivo K_D for Fluo-4 [101], probably the most appropriate Ca^{2+} fluorophore to be used in RBCs [102]. The universal intermediate messenger calmodulin has a dissociation constant for Ca^{2+} of 920 nM [103], which can be shifted down to 100 nM, indicated by the red arrow. The Gárdos channel has an open probability of EC_{50} of 4.7 μM with a Hill slope factor of approximately 1 [104]. Values were measured in excised patches at a membrane potential of 0 mV. The curve of the opening frequency is almost superimposable (EC_{50} of 4.3 μM) [104] keeping the values given in the figure valid also for whole cell and hence population based investigations. The values for half maximal activation of the scramblase was determined by different studies with varying methodologies and a slightly different result. Values varied between approximately 30 μM determined in liposomes [105] and 70 μM measured in RBC ghosts [106]. The flippase displays almost full inhibition already at a Ca^{2+} concentration of 400 nM [107]. μ -Calpain, a protein that cleaves cytoskeleton and membrane proteins depicts an half activation at 40 μM Ca^{2+} [108] but can be activated and then shifting half-maximal activation down to 200 nM [109]. Transglutaminase mediating polymerisation of RBC membrane proteins in its native form has a dissociation constant for Ca^{2+} of 190 μM [110]. Adenosine monophosphate (AMP) deaminase is an enzyme that converts AMP into inosin monophosphate and is directly stimulated by Ca^{2+} at a half maximal concentration of 50 μM free Ca^{2+} [111]. The binding of Ca^{2+} to the C2-domain of PKC α was determined in vitro to be 35 μM with a Hill coefficient of 0.9 [112]. Although the Ca^{2+} dependence of the membrane binding was measured to be one order of magnitude lower [112], the initial Ca^{2+} binding is the crucial step for PKC α activation and therefore the relevant number in this compilation. (This figure is reproduced from Bogdanova et al. 2013 [3])

25.2 The Gárdos Channel – A Calcium-Activated Potassium Channel

The Gárdos channel is one of the Ca^{2+} sensors in RBCs transferring Ca^{2+} uptake into K^+ and water loss and mediating thereby Ca^{2+} -dependent volume regulation and changes in RBC rheology. It is also annotated as KCNN4, $K_{\text{Ca}3.1}$, IK1 or SK4. It is the first channel we describe in this chapter because it was the first channel found in RBCs [22, 23], i.e. utilising the patch-clamp technique as a direct read-out of channel activity. However, its name goes back to the effect of Ca^{2+} dependent

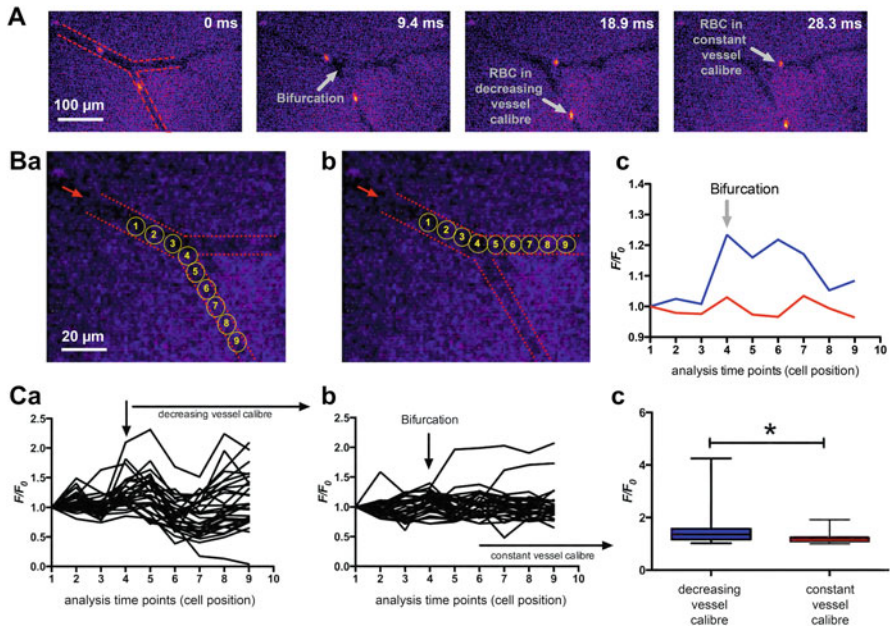


Fig. 25.2 In vivo Ca^{2+} -signalling of mouse RBCs when passing through capillaries. Mouse RBCs were ex vivo stained with Fluo-4 and then re-injected into the mouse circulation. Fluorescence imaging of capillaries was performed in the dorsal skinfold chamber. (A) shows representative snapshots of RBCs passing a bifurcation. For the 30 ms sequence only every second recorded image is presented. For a better orientation the vessel walls are indicated by red dashed lines in the leftmost image and further annotations (grey) are added in the other images. (B) depicts the positions where fluorescence intensity (F/F_0) was analysed for a decreasing vessel calibre (Ba) and for a constant vessel calibre (Bb) of the same example section as in (A). The dashed red lines mark the vessel walls, the red arrow indicates the blood flow direction and the yellow circles depict the analysis positions which are plotted in the following diagrams. Example fluorescence traces of the two cells analysed as pointed out in (Ba) and (Bb) are shown in (Bc). (C) depicts the analysis of 30 cells passing through a capillary with decreasing vessel calibre and 28 cells passing through a capillary with constant vessel calibre. Analysis was performed at 3 vessel-bifurcations in 2 mice. The fluorescence intensity (F/F_0) traces of all measured RBCs passing through a capillary with decreasing vessel calibre is plotted in (Ca), while the traces of all measured RBCs passing a capillary with constant vessel calibre is plotted in (Cb). The statistical analysis of the maximal fluorescence intensity (F/F_0) of RBCs from both groups is depicted in (Cc). The increase in Ca^{2+} , while passing through a vessel with decreasing calibre is significant ($p = 0.014$; *). (This figure is reproduced from Danielczok et al. 2017 [5])

K^+ efflux found in RBCs by G. Gárdos once metabolic pathways are poisoned [24, 25]. As the molecular identity of this transport in RBCs was not known, it was referred to as Gárdos effect and later, when it turned out to be ion channel mediated, the involved transport protein was called Gárdos channel. Even after its molecular identification in 2003 [26] in the RBC field it remained to be referred to as Gárdos channel. Figure 25.3 provides the milestones in the Gárdos channel research. A comprehensive review of the Gárdos channel structure and function was published

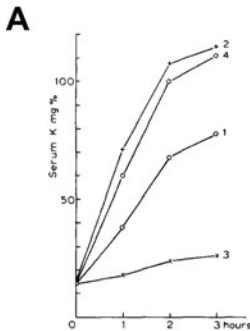


Fig. 2. Effect of CaCl_2 on the K permeability of blood containing IA + adenosine. (37°). 1: $10^{-3} M$ IA + $10^{-2} M$ adenosine; 2: $10^{-3} M$ IA + $10^{-2} M$ adenosine + $5 \cdot 10^{-3} M$ CaCl_2 ; 3: $10^{-3} M$ IA + $10^{-2} M$ adenosine + $2 \cdot 10^{-3} M$ EDTA; 4: $10^{-3} M$ IA + $10^{-2} M$ adenosine + $2 \cdot 10^{-3} M$ EDTA + $5 \cdot 10^{-3} M$ CaCl_2 .

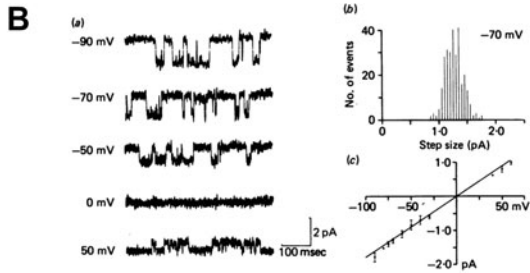


Fig. 1. K-channel currents activated following 'Gárdos treatment'. Cells were preincubated at 37°C for 2-6 hr in mammalian saline containing 1 mM-iodoacetic acid and 10 mM-adenosine. (a) Single channel currents (inward current is downward) recorded from a red blood cell in an external solution containing 100 mM-KCl, 1 mM- CaCl_2 , 1 mM- MgCl_2 , 5 mM-HEPES buffer pH 7.2. The pipette contained the same solution (temp. 19°C). Currents were recorded at different potentials on the same patch by polarizing the pipette. (b) Histogram of current step sizes measured at -70 mV. (c) I-V relationship for currents recorded from five cells (mean \pm s.e. of mean) measured under similar conditions as in a.



Fig. 3. Western blots showing that the protein for the Gardos channel isoform, SK4, is present in cultured human erythroid progenitor cells and in ghost membranes made from mature human red blood cells. The antibody was prepared against an SK4-specific peptide and used as described in *Methods*. The two positive controls are human parotid gland (P) and kidney (K) with the negative control being brain (B). It is clear that a band of the appropriate molecular weight is present in the human erythroid progenitor cells as they mature from days 7 to 13. It is also evident that the SK4 band is present in human red cell ghost membranes (RBC). The decrease in the blot intensity of the D13 band compared with D7 is primarily due to the decreased protein content (cell number) of cells loaded onto the gel. The slight variation in the molecular weights of SK4 bands seen in the progenitor cells, relative to the other bands, may be due to posttranslational modification or higher salt concentration in the loading mixture. It should also be mentioned that, except in the parotid lane, there are higher molecular weight bands (not shown) that in each case react with the antibody. Importantly, preincubation of the antibody with purified peptide that contains the antigenic epitope produces a complete loss of reactivity in all lanes except in brain, where it is much reduced, and in ghosts, where it is only faintly present in the highest molecular weight bands (data not shown).

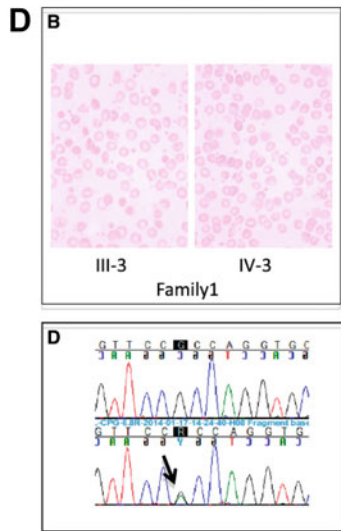


Fig. 25.3 Milestones in Gárdos channel research. (a) Reprint from Gárdos 1958 [25]; a one page article mentioning a dependence of K^+ -efflux from Ca^{2+} in the category "preliminary notes" was retrospectively sufficient for the naming of an ion channel. IA stands for iodoacetic acid. (b) Reprint from Hamill 1981 [23]; the first published single channel current traces from the Gárdos channel appeared in a poster Abstract for the Physiological Society (London) meeting. Numerous patch-clamp based characterisations followed this initial recording [22, 28, 104, 103-107]. (c) Reprint from Hoffman et al. 2003 [26] providing the molecular identification of the Gárdos channel to be KCNN4 ($\text{K}_{\text{Ca}}3.1$, IK1, SK4). (d) Reprint from Rapetti-Maus et al. 2015 [29] providing the first report of a Gárdos channel mutation and its link to a pathophysiological setting. Upper panel: Blood film smears for two patients with the Gárdos channel mutation p.Arg352His (mother and son). Lower panel KCNN4 transcript sequencing; upper line presents the wild type sequence and the lower line the transcript with mutation c.1055G.A (p.Arg352His)

some 15 years ago [27]. An interesting property of the channel is its temperature dependence. With decreasing temperature, a continuous decrease of Gárdos channel conductance is observed. The Arrhenius plot of the unitary channel conductance between 0 °C and 47 °C is strictly linear and has a slope which corresponds to an activation energy of 29.6 ± 0.4 kJ/mol. Nevertheless, simultaneously, altered gating kinetics results in an increase of channel opening probability at reduced temperatures. At saturating concentration of intracellular Ca^{2+} (10 μM), reducing the temperature from 35 to 30 °C results in a change of the opening and closing kinetic of the Gárdos channel. Brief channel openings and closing are progressively replaced by longer openings and shorter closing states [28]. More importantly, reducing the Ca^{2+} concentration at the intracellular face of the channel at half the EC_{50} for Ca^{2+} and temperature close to 0 °C drastically increases open probability indicating that even at very low Ca^{2+} concentrations the Gárdos channel may be activated. Knowing that blood samples for analyses and RBC concentrates for blood transfusion are kept refrigerated, one has to keep in mind this peculiar property of the Gárdos channel that may have deleterious effects respective to the cell volume.

The physiological function of the Gárdos channel was a speculative topic for many decades although a link to RBC cell volume threatening was clear, since activation of the Gárdos channel results in cellular K^+ loss associated with Cl^- and osmotically obliged water loss may lead to rapid cell shrinkage. In this context the channel was believed to be a ‘suicide mechanism’ triggered by the intracellular increase in Ca^{2+} . This was proposed to happen in the process of clot formation, in thrombotic events as well as during RBC clearance. With the finding of the first mutations in the Gárdos channel [29, 30] (see also Fig. 25.3D) and the associated pathophysiology, a physiological function of the Gárdos channel was doubtless proven. Although the initial reports link the mutation of the Gárdos channel to Hereditary Xerocytosis [29, 30], further studies revealed that ‘Gárdos channelopathy’ is its own disease or at least an own variant of Hereditary Stomatocytosis [31]. Any prolonged Gárdos channel activation lead to changes in cell volume which eventually affect rheological, stiffness and rigidity properties that compromise their survival within the circulation especially during their passage within the slits of the spleen. The mutations reported so far resulted in a gain of function that could be treated with a Gárdos channel inhibitor. There are numerous Gárdos channel inhibitors available some of them already clinically tested for other diseases, like clotrimazole for topical applications or senicapoc [32]. The Gárdos channel also shows an increased activity in other haemolytic diseases, such as sickle cell disease. Therefore one has tried to use the Gárdos channel as a pharmacological target to treat sickle cell disease [33] overlooking the fact that upstream of the signalling cascade is an increase in intracellular Ca^{2+} through a pathway named P_{sickle} for which we are still seeking molecular identity (see below) and triggers numerous other pathophysiological processes in the RBCs (compare Fig. 25.1) leaving the Gárdos channel only a minor portion to account for the cellular symptoms of sickle cell disease [34]. However, what failed in sickle cell disease may still work out well in Gárdos Channelopathy [31, 35].

25.3 Non-selective Cation Channels Permeable for Calcium

25.3.1 Non-selective Voltage Dependent Cation Channel and Piezo1

RBCs contain a variety of non-selective ion channels that are permeable to Ca^{2+} . First there is a non-selective voltage dependent cation channel initially described by Christophersen and Bennekou [36, 37] and later to be reported to be Ca^{2+} permeable [38]. However, the molecular identity of this channel is still not quite clear [39, 40]. Although it was proposed to be a conductive state of the voltage-dependent anion channel (VDAC) [41], recent reports rather make a link to the Piezo1 [42, 43]. Figure 25.4 provides a comparison of the non-selective voltage dependent cation channel and Piezo1. The unique hysteresis-like open probability was also modelled successfully [44].

PIEZO1 and in particular mutations of the channel have been associated with the RBC-related disease Hereditary Xerocytosis [45, 46]. Therefore it seems obvious that this channel, originally described as a mechanosensitive channel, is present in the RBC membrane. Furthermore, knock-out approaches in zebrafish [21] and mice [20] gave further evidence for the conserved abundance of Piezo1 in RBCs as well as for its function (see below). Piezo1 and its mutations were mainly characterised in heterologous overexpressing cell lines and initial measurements of Piezo1 in RBC have been rather episodic [47]. However, the discovery of the pharmacological activation of Piezo1 by Yoda1 [48] lead to the development of high throughput patch-clamp assays as potential diagnostic tools that were recently implemented [49].

The interplay of Piezo1 (in particular its property to mediate Ca^{2+} entry) with the above mentioned Gardos channel [5, 20, 21] provides additional evidence for a functional Piezo1 in RBCs. Furthermore, the interplay between the channels was proposed to be vital for the RBCs to maintain their ion homeostasis [50]. In pathophysiology, Piezo1 seems to play a mayor role in an increased RBC Ca^{2+} -homeostasis. The reported mutations of Piezo1 [45, 46, 51–54] are mostly gain of function mutations suggesting an easier and more pronounced Ca^{2+} entry. The consequent increase in intracellular Ca^{2+} is most likely the trigger for the early removal of the RBC from the circulation and hence the reason for the anaemic symptoms [55]. One of the clinical treatments to handle severe anaemias is splenectomy. Interestingly splenectomy introduces comorbidity, namely thrombotic events, in a subpopulation of Hereditary Xerocytosis patients. This could be explained by an active participation of RBCs in the thrombus formation due to increased intracellular Ca^{2+} [13, 14, 56–58]. Surprisingly such thrombotic events were not reported for splenectomised Gárdos Channelopathy patients [31].

It is worthwhile to mention that in sickle cells an increased conductance carrying also Ca^{2+} was reported and named P_{sickle} [59, 60]. It is likely that P_{sickle} resembles the superposition of several ion channel entities. The sensitivity of P_{sickle} to GsMTx-4 [61], a toxin that inhibits Piezo1 [62] points to this mechanosensitive channel, while the increased abundance of *N*-methyl-D-aspartate (NMDA) receptors in sickle cells [63] is a very strong indicator for these ionotrope glutamate receptors (see below).

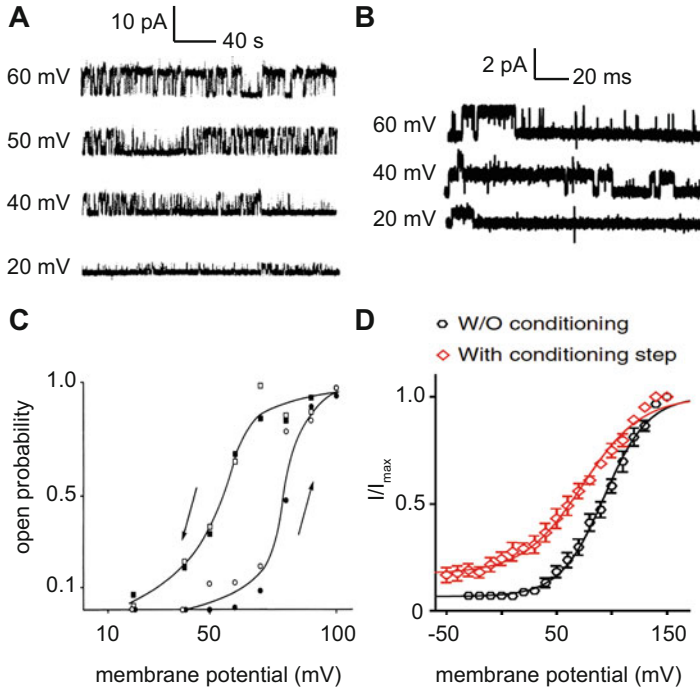


Fig. 25.4 Comparison of the non-selective voltage activated cation channel recorded in RBCs and Piezo1 recorded in overexpressing Neuro2A cells. (a) Current traces of the non-selective voltage activated cation channel in inside-out patches of RBCs in symmetrical KCl-solution in mM (500 KCl, 5 MOPS, 4 NMDG, 1 EGTA, 0.02 Ca^{2+} , pH = 7.4). (b) Current traces of Piezo1 in outside-out patches of overexpressing Neuro2A cells in symmetrical NaCl-solution in mM (140 NaCl, 10 HEPES, 5 EGTA, pH = 7.4). The difference in ion strength between panels a and b could explain the different current amplitudes shown in the single channel openings. (c) The open state probability as function of the membrane potential. Filled symbols represent data from the experiment shown panel a. Open symbols represent data from an identical experiment performed on the same patch after 15 min. In both series, the open probability was calculated from 3 min of continuous recording at each potential. The curves were drawn by eye. (d) Tail currents from individual cells were normalized to their maximum and fitted to a Boltzmann relationship. Pooled data are shown as mean \pm SEM. (Panels a and c are reproduced from Kaestner et al. 2000 [38] and panels b and d from Moroni et al. 2018 [42])

25.3.2 N-Methyl D-Aspartate Receptor

There is clear evidence for the abundance of erythroid N-methyl D-aspartate (NMDA)-receptors in RBCs in particular in the young cell population [19, 64, 65] and its abnormally high prevalence and activity in sickle cell patients [34, 63]. Inhibition of these receptors by oral administration of memantine, the pore-targeting antagonist of NMDARs, results in a decrease of the intracellular Ca^{2+} (Fig. 25.5). In general, cells stemming from myeloid lineage are expressing

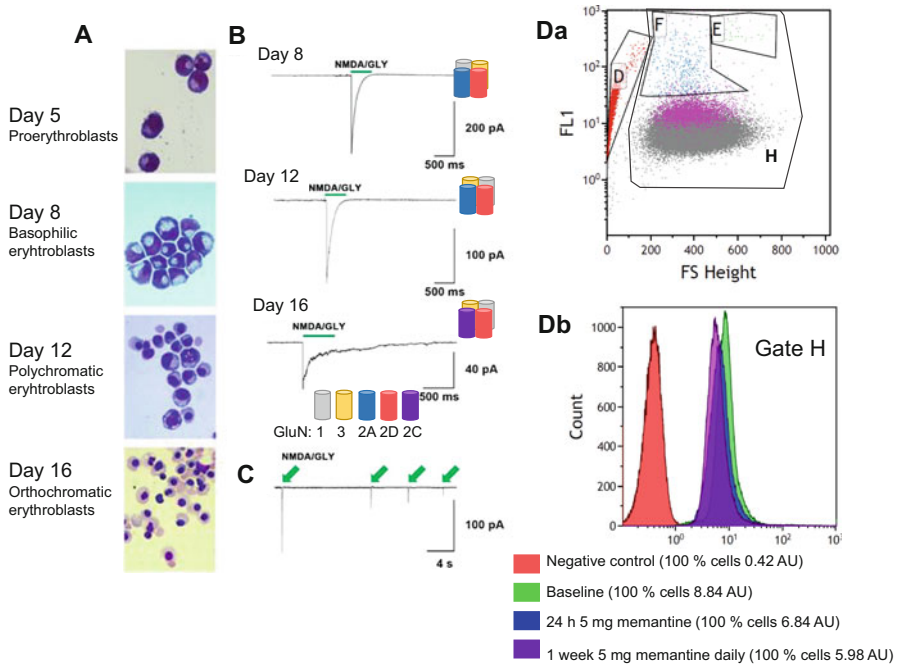


Fig. 25.5 NMDA receptors structure and function. (A) Erythroid NMDA receptors are expressed early on in differentiating erythroid progenitor cells starting from proerythroblasts (CD34 + -derived cells on day 5 in culture) to orthochromatic erythroblasts (day 16 in culture). (B) Electrophysiological recordings of currents mediated by treatment of these cells with agonists NMDA and glycine reveal the change in subunit composition of the receptor during differentiation. Whereas proerythroblasts and polychromatic erythroblasts are equipped with receptors built by glycine-binding GluN1 and 3A/B and glutamate/NMDA-binding GluN2A and 2D (see cartoons), late orthochromatic erythroblasts and reticulocytes contain receptors in which GluN2A is replaced by GluN2C. As a result channels with high current amplitudes and short times to inactivation in early progenitors turn into slowly inactivating channels with lower amplitude in late progenitors and circulating RBCs. For details see [67]. (C) Repeated activation of eNMDARs triggers inactivation of the channels. (D) Changes in the intracellular Ca^{2+} concentration in RBCs upon systemic administration of memantine in patients with sickle cell disease. (Da) Dot plot showing the heterogeneity of free Ca^{2+} levels in RBCs (gates F, E, and H) and RBC-derived vesicles (gate D). (Db) shows a histogram of Ca^{2+} -dependent fluorescence (all cells in population, gate H) in unstained cells (negative control, red), at baseline before the onset of treatment with 5 mg memantine a day (green) after 24 h (blue) and 1 week (pink) of therapy with 5 mg Memantine Mepha daily. The treatment was performed within the MemSID clinical trial ([ClinicalTrials.gov Identifier: NCT02615847](https://clinicaltrials.gov/ct2/show/study/NCT02615847) approved by SWISSMEDIC (# 2015DR2096) and Cantonal ethic committee of canton Zurich (#2015-0297)). (Panels A–C are reproduced from Hänggi et al. 2015 [67] and panel D from Makhro et al. 2017 [66])

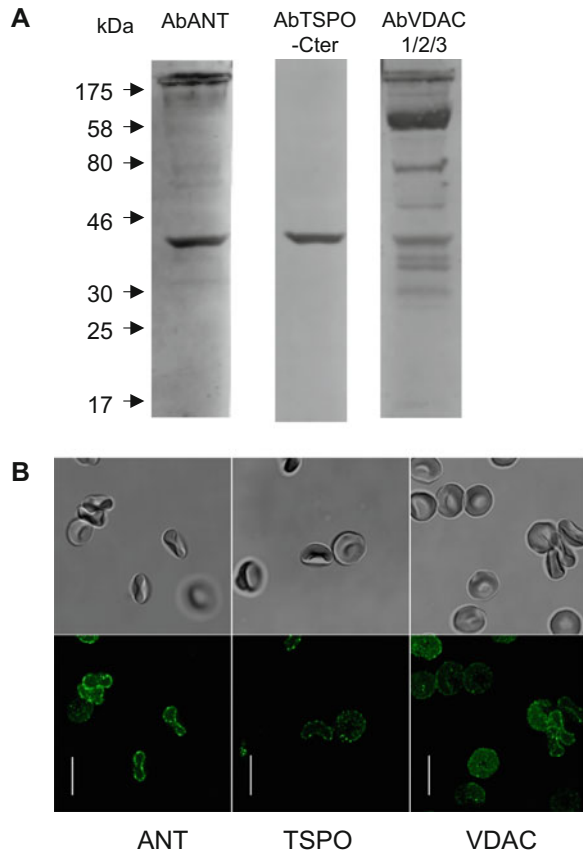
particular type of ionotropic glutamate receptors making immune responses, clotting and RBC function sensitive to the changes in ambient glutamate levels [66]. Subunit composition of erythroid NMDA receptors (eNMDARs) as well as the number of receptor copies changes in the course of differentiation (Fig. 25.5A–C).

Receptor abundance declines from thousand copies in proerythroblasts to about 30 in reticulocytes and about 5 (on average) in mature RBCs [19, 67]. At the same time high amplitude currents with short inactivation time carried by the GluN2A/2D-containing receptors in proerythroblasts are replaced by the currents mediated by the receptors built by the GluN2C/2D subunits with much smaller amplitude and prolonged inactivation time in ortho/polychromatic erythroblasts and reticulocytes [67], (Fig. 25.5A–C). eNMDARs are highly permeable for Ca^{2+} [19, 64] and are actively involved in Ca^{2+} -driven signaling during differentiation and maintenance of intracellular Ca^{2+} in mature RBCs [19, 67]. Clearance of eNMDARs in reticulocytes released into the circulation most likely occurs by way of ‘shedding’ when receptors are released together with other membrane proteins from the membrane in the form of vesicles. Whereas no direct measurements of eNMDARs in vesicles were performed so far, inability to clear eNMDARs from membranes of RBCs of patients with sickle cell disease is an indirect evidence for this hypothesis. In erythroid precursor cells obtained by differentiation of peripheral CD34+ cells of sickle cell disease patients the number of eNMDAR copies was like that in cells of healthy patients [67]. However, circulating RBCs of patients were presented with abnormally high abundance and activity levels of eNMDARs. As a result, basal Ca^{2+} levels in RBCs of sickle cell disease patients were exceeding that in cells of healthy subjects. Pharmacological inhibition of the receptors decreased Ca^{2+} levels and resulted in rehydration and reduction in oxidative load [67]. First pilot clinical trial MemSID in which patients with sickle cell disease were treated with the antagonist of NMDA receptors, memantine, revealed that these receptors may be an attractive pharmacological target for this group of patients [68, 69] (Fig. 25.5D). Among physiological factors that may control eNMDARs are endurance exercises that are associated with glutamate release into the circulation [70].

25.3.3 Voltage-Dependent Anion Channel

Another multifunctional channel with a clear molecular identity in RBCs that also conducts Ca^{2+} is the Voltage-Dependent Anion Channel (VDAC) [41, 71]. VDACS have originally been characterized as mitochondrial porins [72]. Three different isoforms of VDAC have been identified so far: VDAC1, VDAC2 and VDAC3. Showing the expression of ‘Porin 31HL’ in the plasmalemma of human B lymphocytes, gave first evidence on the multitopological localisation of VDAC [73]. The existence in the membrane of RBCs of a 32 kDa associated voltage dependent anion channel (VDAC) in a peripheral benzodiazepine receptor-like PBR protein complex to 18 kDa protein TSPO ‘translocator proteins’ and 30 kDa ANT ‘adenine nucleotide transporter’ proteins has been demonstrated [41, 74]. It has a nanomolar affinity for PK11195, Ro5–4864 and Diazepam ligands [75,

Fig. 25.6 VDAC, ANT and TSPO detection in human red blood cell ghosts. **(a)** Samples (15 μ g of protein) of whole lysates were subjected to SDS-PAGE (10% acrylamide) and analysed by Western blotting using polyclonal anti-ANT (1:1000 dilution), polyclonal goat anti-TSPO raised against the C terminus of human TSPO (1:1000) or rabbit polyclonal anti VDAC 1–2–3 (1:100 dilution). Multiple bands at different molecular weights is consistent with the oligomerisation of VDAC proteins. ANT and TSPO proteins are also clearly visible. **(b)** Immunofluorescence experiments were performed on smears Dilution were 1/5 for primary and 1/20 for secondary antibodies. Scale bars represent 10 μ m. (This figure is reproduced from Bouyer et al. 2011 [41])



76]. All blood cells have a population of receptors with micromolar affinity for PK11195 ranging from approximately 750,000 sites for lymphocytes to over one hundred sites for RBCs [77, 78]. These indications are corroborated by analysis of messenger RNA expression data provided by GeneAtlas U133A where 3 isoforms of VDAC, 2 isoforms of ANT and 2 isoforms of TSPO were found in erythroid progenitors from CD34+ to CD71+ (Fig. 25.6). VDAC is a protein that has remarkably well-preserved structural and functional characteristics, despite major variations in the sequence [79]. Although it is also present in the plasma membrane, most of the information we have on its structure function comes from studies on mitochondrial proteins [80, 81]. The maximum conductances reach 4–5 nS in the

presence of 1 M NaCl or KCl, 350–450 pS for more physiological concentrations (NaCl or 150 mM KCl). Conductance and selectivity are voltage dependent; at low voltages, close to -10 mV, the channel is stable and remains open, whereas at positive or negative potentials higher than 40 mV, VDAC has multiple sub states of different permeabilities and selectivities, as well as closing episodes of which frequency increases with voltage [82, 83]. The highest levels are permeable to small ions (Na^+ , K^+ , Cl^- , etc.) but also to large anions (glutamate, ATP) and large cations (acetylcholine, dopamine, Tris, etc.). They have a preference for anions (2:1) when saline solutions are composed of ions of equal mobility such as NaCl or KCl. More importantly, at low conductances, VDAC is more permeable to small ions with, apparently, a marked preference for cations and higher permeability to Ca^{2+} ions than in large conductances [82–84]. VDAC may have different oligomerization states: mono-, di-, tri-, tetra-, hexamers or even more. Indeed, atomic force microscopy revealed the presence of VDAC1 monomers as well as dimers and larger oligomers showcasing the interaction of the pore with itself, however, dimers are more frequent. Very little is known about the activation and regulation mechanisms of the channel. Nevertheless, when the pores dimerize, the selectivity for Ca^{2+} increases. Various studies support the function of VDAC (more precisely VDAC1 the most studied yet) in the transport of Ca^{2+} and in cellular Ca^{2+} homeostasis. Lipids-reconstituted bilayer incorporating VDAC1 in the presence of different CaCl_2 concentration gradients showed well-defined voltage-dependent channel conductance, as observed with either NaCl or KCl solution, with higher permeability to Ca^{2+} once VDAC is in the low conductance state. It is obvious that the permeability ratios of VDAC1 for Ca^{2+} is very low compared to Cl^- ($P_{\text{Ca}^{2+}}/P_{\text{Cl}^-}$ is 0.02–0.38) [83] but considering the tremendous electrochemical gradient for Ca^{2+} between intra- and extracellular face of RBCs (see Introduction) a short activation may represent a significant input of Ca^{2+} into the cell.

25.3.4 Transient Receptor Potential Channels of Canonical Type

Yet another type of non-selective cation channels that are believed to be abundant in RBCs are Transient Receptor Potential channels of Canonical type (TRPC channels). Indications point to a different expression pattern of isoforms in precursor cells compared to mature RBCs and also differences between mammalian species seem likely [85–88]. In humans it is believed that TRPC6 is abundant in RBCs [39, 89, 90]. So far a dedicated physiological function of TRPC6 in mature RBCs remains elusive.

25.4 Voltage-Activated Calcium Channels and Their Regulation

Evidence for the existence of a number of voltage-activated Ca^{2+} channels in RBCs has been reported [91, 92], and the most convincing evidence is for $\text{Ca}_V2.1$, based on molecular biology data (Western blot) [93] and, presumably, $\text{Ca}_V2.1$ -specific pharmacological interactions (ω -agatoxinTK) [93, 94] – both are shown in Fig. 25.7A, B. Nevertheless, so far, we and others have failed to obtain direct functional evidence for the existence of $\text{Ca}_V2.1$ or other voltage-activated Ca^{2+} channels in RBCs by patch-clamp techniques [95]. However, also RBCs although non-excitabile cells meet the condition of voltage jumps necessary to activate voltage-activated channels such as $\text{Ca}_V2.1$ [95]. In particular when the Gárdos channel (see Sect. 25.2) is activated, the resting membrane potential changes from approximately -10 mV to approximately -70 mV [96]. Not hyperpolarisation but depolarisation is required to activate $\text{Ca}_V2.1$ [97]. Nevertheless, hyperpolarisation is a requirement to switch $\text{Ca}_V2.1$ channels from the inactivated state to the closed state, which is a prerequisite to subsequently transition to the open state [98] (Fig. 25.7C). Closing of the Gárdos channels after their initial activation could well provide the necessary conditions for subsequent depolarisation to activate $\text{Ca}_V2.1$ [95]. Such a proposed mechanism is sensible also in the context of other voltage-activated channels in the RBC membrane (compare Sect. 25.3).

25.5 Evidence for a Calcium-Inhibited Channel

There is also evidence for a non-selective cation channel in RBCs that is activated when extracellular Ca^{2+} is removed [99]. Original recordings and an I–V curve are shown in Fig. 25.8A, B. There are two conceptual questions related to this recent report (a) if the channel is abundant in almost all RBCs why it was not reported before (in four decades of patch-clamping RBCs) and (b) since divalent cations in general and Ca^{2+} in particular support seal formation, a removal of Ca^{2+} could impair the seal quality/tightness. Under these circumstances it is almost impossible to discriminate a leak in the seal from an ion channel. However, here are also two arguments in favour of the existence of this channel: (A) The suspicion of the phenomenon described in (b) could have prevented scientists to report about the channel (a). The non-ohmic behaviour of the I–V curve (Fig. 25.8B) is in favour of a channel rather than a leak. (B) A channel activated by the removal of Ca^{2+} is an ideal explanation of the dissipation of the monovalent cation gradients when

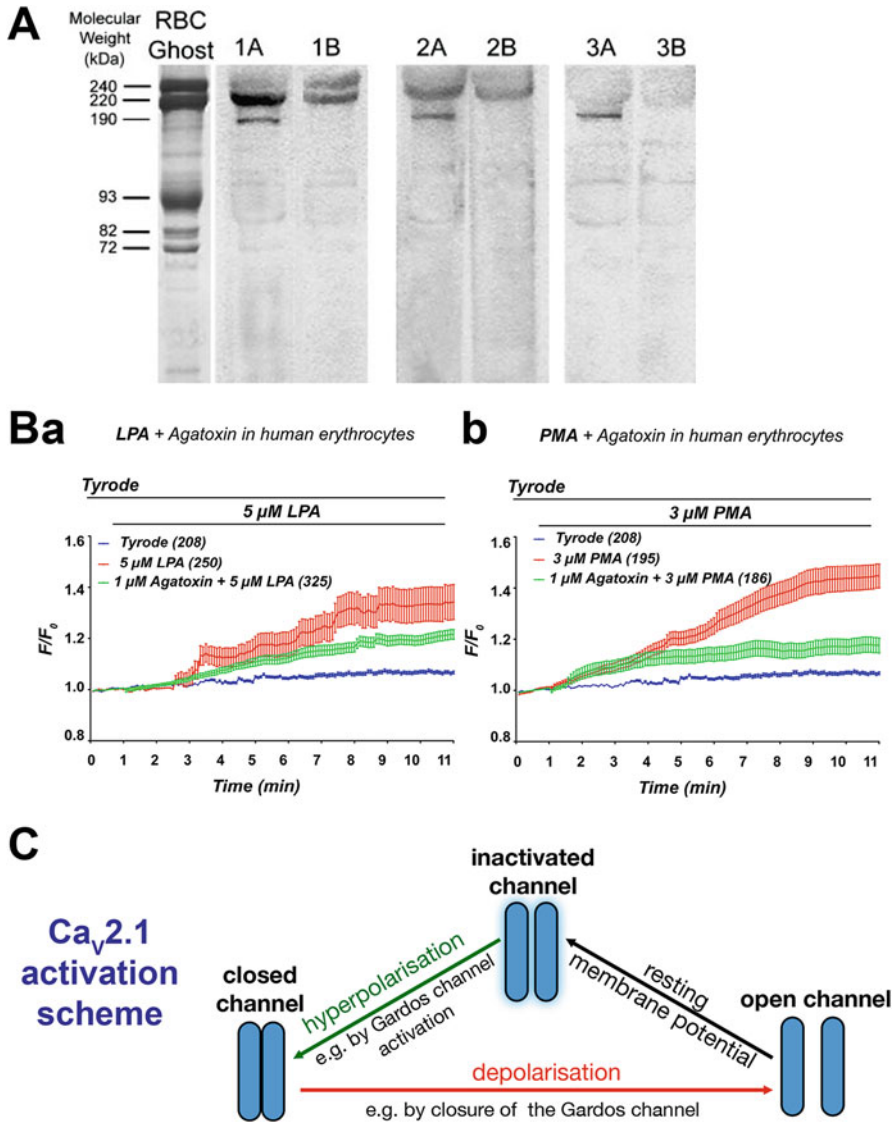


Fig. 25.7 Ca_v2.1 in human RBCs. (A) Western blot analysis of the 1A subunit of voltage-gated calcium channels in human erythrocyte ghosts from 3 different donors. RBC membrane proteins were separated electrophoretically at high protein loads (80 μg). After electrophoretic transfer to nitrocellulose paper, blots were stained with antibodies directed against residues 865 to 881 of the α_{1A} subunit of the rat brain voltage-gated calcium channel (lanes 1A, 2A, 3A). Because several nonspecific bands were also visualized, competition of Ca_v2.1 antibody staining using its specific peptide was also performed. For this purpose, 10 μg of the Ca_v2.1 antibody was preincubated with 10 μg of antibody-specific peptide for 1 h at 22 °C and then further incubated with the blot for 2 h at 22 °C (lanes 1B, 2B, 3B). Polypeptides with M_r of approximately 190,000 and 220,000 are characteristic of the major splicing variants of the α_{1A} subunit of Ca_v2.1 in the brain. An SDS-PAGE Coomassie blue–stained gel of RBC membranes (left lane; “RBC Ghost”) serves as an

cells are placed in tubes containing Ca^{2+} -chelating anticoagulants as exemplified in Fig. 25.8C. This experimental result is a showcase of the cation gradient dissipation associated with RBC storage lesions [100].

Fig. 25.7 (continued) approximate molecular weight marker. (B) Kinetics of lysophosphatidic acid (LPA; phospholipid released by activated platelets)-induced (Ba) and Phorbol 12-myristate 13-acetate (PMA; protein kinase C activator)-induced (Bb) Ca^{2+} entry in the presence and absence of ω -agatoxin TK. Average traces of single cells derived from live cell imaging experiments are presented as self-ratio values. Labelled lines above the traces indicate the stimulation regime. The traces are the mean values of 3 independent experiments, and the numbers in brackets at the end of the colour legend refer to the number of cells measured. (C) Activation scheme for the $\text{Ca}_V2.1$ channel modulated by underlying Gardos channel activity. Closing of the Gardos channels after their initial activation could provide the necessary conditions for subsequent depolarisation to activate $\text{Ca}_V2.1$. Since the hypothetical switching behaviour of the Gardos channel would be crucial for the activation of $\text{Ca}_V2.1$, we propose three principle modes by which this switching could occur: (i) Because channel activity is a stochastic event and because the number of Gardos channels per RBC is rather low (in the single digit numbers [114, 118]), depolarisation could be the result of stochastic Gardos channel closures. This hypothesis is supported by the rather sparse whole cell patch-clamp recordings of Gardos channel activity in human RBCs [31, 119–121]. Whole cell current traces do not show a smooth appearance but rather a flickering pattern similar to that observed with single channel recordings, especially at higher (positive and negative) membrane potentials. (ii) When looking at Gardos channel-induced changes in the membrane potential of cell populations, a gradual Ca^{2+} concentration-dependent effect can be seen [122], i.e., the hyperpolarisation observed in RBC suspensions is a gradual Ca^{2+} concentration-dependent effect. However, the abovementioned study [122] as well as another report [123] showed that the activation of the Gardos channel at the cellular level is an all-or-none response. This means that the gradual change in membrane potential would be the result of the summation of cells with open or closed Gardos channels. Taking into consideration that the Ca^{2+} pump [124] continuously operates in response to any increase in intracellular Ca^{2+} levels, one would imagine that the state of the Gardos channels is exclusively modulated by variations in intracellular Ca^{2+} concentrations. Hence, the switching behaviour of the Gardos channel would be the direct consequence of continuous variations in RBC intracellular Ca^{2+} concentrations. (iii) Localized interactions between the Gardos channel and $\text{Ca}_V2.1$ in RBCs could occur in lipid rafts or nanodomains, as is the case with closely related ion transporters in other cell types, for example, within the fuzzy space or dyadic cleft in myocytes [125]. Although RBCs do not possess membrane-constricted subspaces, there are indications for functional compartments in the immediate vicinity of the plasma membrane [126]. Colocalization of ion channels is common in excitable cells [127, 128]. For RBCs, it is still unknown if the different ion channels colocalize or cluster to allow their interaction in nanodomains. However, in support of this idea is the observation that local activation of mechanosensitive channels (most likely Piezo 1) by patch-clamp micropipettes resulted in local activation (single-channel recordings) of the Gardos channel [124]. (Panels A, B and C are reproduced from Andrews et al. 2000 [93], Wagner-Britz et al. 2013 [94] and Kaestner et al. 2018 [95], respectively)

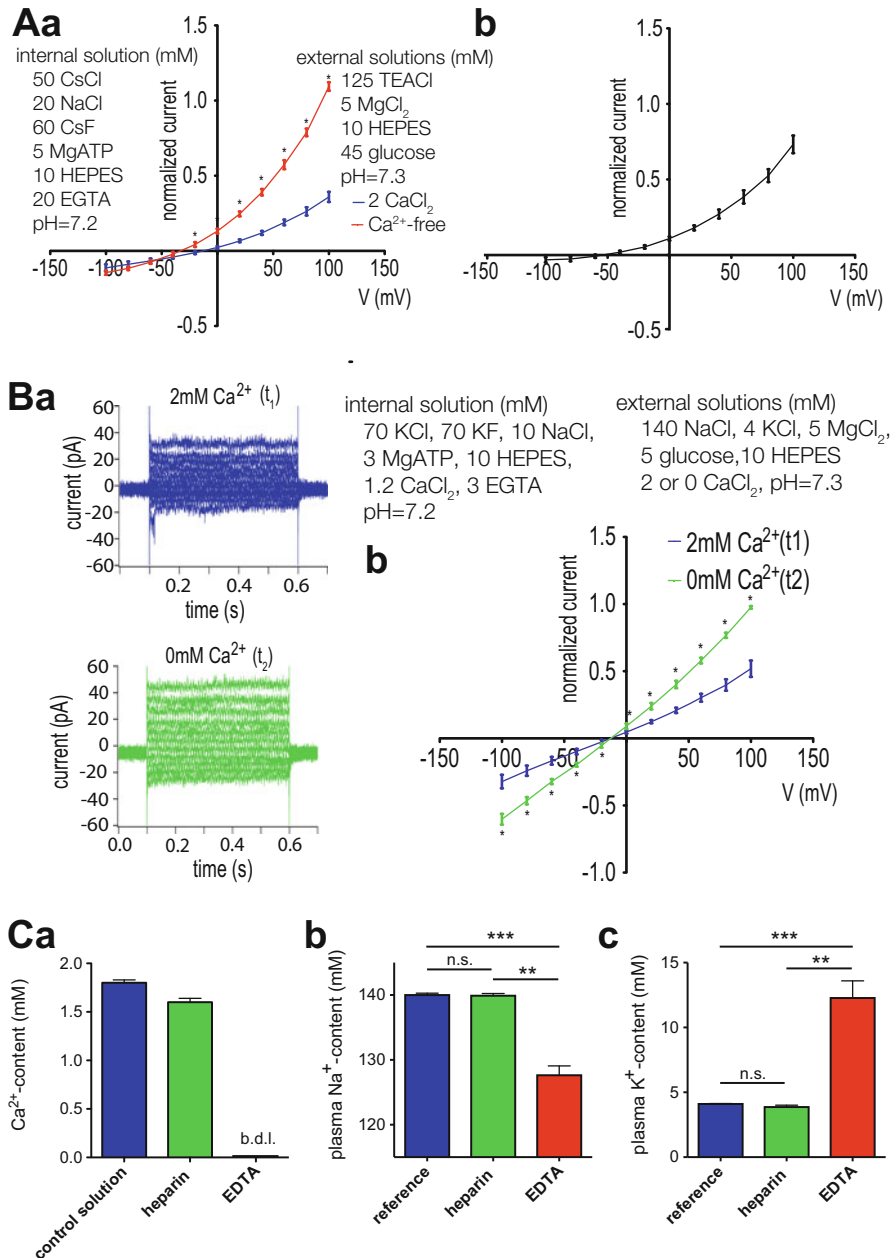


Fig. 25.8 Evidence for non-selective cation channel activated by the removal of Ca²⁺. (A) Whole-cell patch clamp recordings in a Cs⁺-based internal and a TEACl-based external solutions (Aa) I/V curves with 2 mM CaCl₂ (blue) and 0 mM CaCl₂ (red) in the external solution (n = 5). (Ab) I/V curve of the Ca²⁺ blocked current – the current recorded in 2 mM CaCl₂-external solution was subtracted from the current recorded in 0 mM CaCl₂-external solution. Currents were elicited

25.6 Summary

The importance of Ca^{2+} in the membrane transport regulation and mediation of RBCs was early recognised. However, only in the recent years it became evident how this ion transport is related to ion channels and a correlation to molecular entities could be performed. This process is everything but finished and in particular the understanding of the interaction of several ion channels in a physiological context just started. This includes also pathophysiological conditions, on the one hand channelopathies, where a mutation of the ion channel is the direct cause of the disease, like the above described Hereditary Xerocytosis [45] and the Gárdos Channelopathy [31]. On the other hand it applies to RBC related diseases where an altered channel activity is a secondary effect like in sickle cell disease [34, 63] or thalassemia. Also these secondary effects should receive medical and pharmacologic attention because they can be crucial when it comes to the life-threatening symptoms of the disease [55]. An overview of the involvement of Ca^{2+} and Ca^{2+} -conducting channels as general components in anaemias is summarised in Fig. 25.9. However, this scheme can only be regarded as a current snapshot of our knowledge about Ca^{2+} and Ca^{2+} -conducting channels in RBCs. Further investigations on a better match between functional and molecular knowledge will arise as well as a better understanding of the activity of Ca^{2+} and Ca^{2+} -conducting channels within the signalling networks in RBCs.

←

Fig. 25.8 (continued) by voltage steps from -100 mV to 100 mV for 500 ms in 20 mV increments at $V_h = -30$ mV. Detailed solutions composition is given next to the graphs. Data are presented as mean \pm SEM, with n being the number of cells. Significance is assessed with a paired Student's t test and set at $p < 0.05$. For better visualization, a significance anywhere below $p < 0.05$ is denoted with one star. (B) Whole-cell patch clamp recordings in physiological (a K^+ -based internal and a Na^+ -based external) solutions (Ba) Raw current traces from a representative RBC in an external solution containing 2 mM CaCl_2 at t_1 (dark blue) and 0 mM CaCl_2 at t_2 (green). Detailed solutions composition is given next to the current traces. (Bb) I/V curves in 2 mM CaCl_2 (t_1) (dark blue) and 0 mM CaCl_2 (t_2) (green) external solutions ($n = 7$). (C) Blood plasma ion content of healthy adults in heparin and EDTA. (Ca) Ca^{2+} content of a control aqueous non-buffered 1.8 mM CaCl_2 solution filled in heparin and EDTA vacutainers. The abbreviation b.d.l. denotes 'below detection limit'. (Cb) Na^+ plasma content, (Cc) K^+ plasma content of blood anticoagulated with heparin and EDTA. Measurements in heparin and EDTA were performed on blood of healthy adults ($n = 3$) collected in heparin and EDTA vacutainers, respectively and reference values were taken from Liappis, 1972 [130]. Error bars represent SEM and stars denote significances as follows: n.s for not significant, ** for $p < 0.01$ and *** for $p < 0.001$. (This figure is reproduced from Petkova-Kirowa et al. 2018 [99])

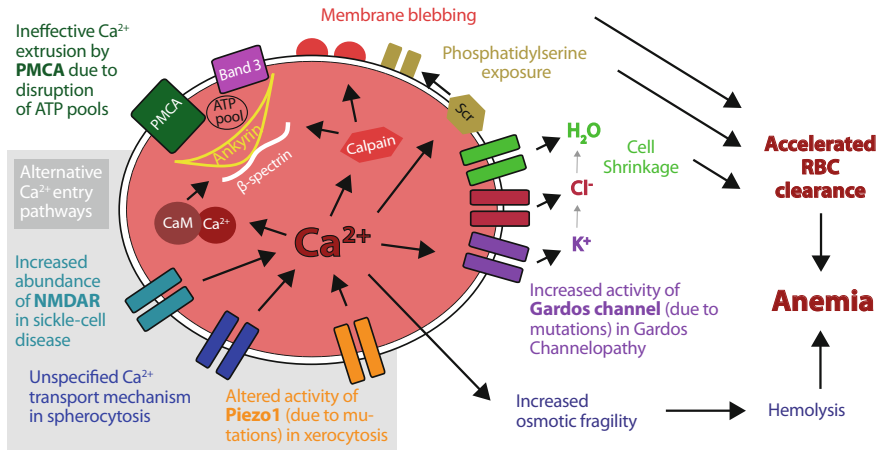


Fig. 25.9 Proposed mechanisms leading to increased intracellular Ca²⁺ levels in diseased RBCs and accordingly to accelerated clearance of cells from the blood stream. Alternative or cumulating Ca²⁺ entry pathways are highlighted with grey background: increased abundance of NMDA-receptors (NMDAR), e.g., in sickle cell disease, altered activity of Piezo1, e.g. in Hereditary Xerocytosis, increased activity of Gárdos Channel, e.g. in Gárdos Channelopathy, or unspecified Ca²⁺ transport mechanisms in spherocytosis. Additionally, ineffective extrusion of Ca²⁺ due to disruption of ATP pools fueling the plasma membrane Ca²⁺ ATPase (PMCA) can contribute. Several downstream processes follow Ca²⁺ overload in RBCs, e.g.: activation of calmodulin by formation of the Ca²⁺-calmodulin complex (Ca-CaM) and activation of calpain, thereby loosening the cytoskeletal structure; activation of the scramblase (Scr) leading to exposure of phosphatidylserine on the outer leaflet of the membrane; activation of the Gárdos channel followed by the efflux of K⁺, Cl⁻ and H₂O and consecutive cell shrinkage. (This figure is reproduced from Hertz et al. 2017 [55])

References

- Berridge MJ (1994) The biology and medicine of calcium signalling. *Mol Cell Endocrinol* 98:119–124
- Berridge MJ (2006) Calcium microdomains: organization and function. *Cell Calcium* 40:405–412
- Bogdanova A, Makhro A, Wang J et al (2013) Calcium in red blood cells—a perilous balance. *Int J Mol Sci* 14:9848–9872. <https://doi.org/10.3390/ijms14059848>
- Lew VL, Tsien RY, Miner C, Bookchin RM (1982) Physiological [Ca²⁺]_i level and pump-leak turnover in intact red cells measured using an incorporated Ca chelator. *Nature* 298:478–481
- Danielczok JG, Terriac E, Hertz L et al (2017) Red blood cell passage of small capillaries is associated with transient Ca²⁺-mediated adaptations. *Front Physiol* 8:979. <https://doi.org/10.3389/fphys.2017.00979>
- Hammer K, Ruppenthal S, Viero C et al (2010) Remodelling of Ca²⁺ handling organelles in adult rat ventricular myocytes during long term culture. *J Mol Cell Cardiol* 49:427–437. <https://doi.org/10.1016/j.yjmcc.2010.05.010>
- Schatzmann HJ (1983) The red cell calcium pump. *Annu Rev Physiol* 45:303–312. <https://doi.org/10.1146/annurev.ph.45.030183.001511>
- Scharff O, Foder B (1977) Low Ca²⁺ concentrations controlling two kinetic states of Ca²⁺-ATPase from human erythrocytes. *Biochim Biophys Acta* 483:416–424

9. Kosk-Kosicka D, Bzdega T (1990) Effects of calmodulin on erythrocyte Ca^{2+} -ATPase activation and oligomerization. *Biochemistry* 29:3772–3777
10. Wang KK, Roufogalis BD, Villalobo A (1990) Calpain I activates Ca^{2+} transport by the human erythrocyte plasma membrane calcium pump. *Adv Exp Med Biol* 269:175–180
11. Wang KK, Villalobo A, Roufogalis BD (1992) The plasma membrane calcium pump: a multiregulated transporter. *Trends Cell Biol* 2:46–52
12. Kosk-Kosicka D, Bzdega T (1988) Activation of the erythrocyte Ca^{2+} -ATPase by either self-association or interaction with calmodulin. *J Biol Chem* 263:18184–18189
13. Andrews DA, Low PS (1999) Role of red blood cells in thrombosis. *Curr Opin Hematol* 6:76–82
14. Kaestner L, Tabellion W, Lipp P, Bernhardt I (2004) Prostaglandin E2 activates channel-mediated calcium entry in human erythrocytes: an indication for a blood clot formation supporting process. *Thromb Haemost* 92:1269–1272. <https://doi.org/10.1267/THRO04061269>
15. Lang KS, Duranton C, Poehlmann H et al (2003) Cation channels trigger apoptotic death of erythrocytes. *Cell Death Differ* 10:249–256. <https://doi.org/10.1038/sj.cdd.4401144>
16. Kaestner L, Minetti G (2017) The potential of erythrocytes as cellular aging models. *Cell Death Differ* 24:1475–1477. <https://doi.org/10.1038/cdd.2017.100>
17. Lang KS, Lang PA, Bauer C et al (2005) Mechanisms of suicidal erythrocyte death. *Cell Physiol Biochem* 15:195–202
18. Galluzzi L, Vitale I, Aaronson SA et al (2018) Molecular mechanisms of cell death: recommendations of the Nomenclature Committee on Cell Death 2018. *Cell Death Differ*:1–56. <https://doi.org/10.1038/s41418-017-0012-4>
19. Makhro A, Hanggi P, Goede JS et al (2013) N-methyl D-aspartate (NMDA) receptors in human erythroid precursor cells and in circulating red blood cells contribute to the intracellular calcium regulation. *Am J Physiol Cell Physiol*. <https://doi.org/10.1152/ajpcell.00031.2013>
20. Cahalan SM, Lukacs V, Ranade SS et al (2015) Piezo1 links mechanical forces to red blood cell volume. *Elife* 4:e07370. <https://doi.org/10.7554/eLife.07370>
21. Faucher A, Kissa K, Nargeot J et al (2014) Piezo1 plays a role in erythrocyte volume homeostasis. *Haematologica* 99:70–75. <https://doi.org/10.3324/haematol.2013.086090>
22. Hamill OP (1983) Potassium and chloride channels in red blood cells. In: Sakmann B, Neher E (eds) *Single channel recording*. Plenum Press, New York/London, pp 451–471
23. Hamill OP (1981) Potassium channel currents in human red blood cells. *J Physiol Lond* 319:97P–98P
24. Gardos G (1956) The permeability of human erythrocytes to potassium. *Acta Physiol Hung* 10:185–189
25. Gardos G (1958) The function of calcium in the potassium permeability of human erythrocytes. *Biochim Biophys Acta* 30:653–654
26. Hoffman JF, Joiner W, Nehrke K et al (2003) The hSK4 (KCNN4) isoform is the Ca^{2+} -activated K^+ channel (Gardos channel) in human red blood cells. *Proc Natl Acad Sci U S A* 100:7366–7371. <https://doi.org/10.1073/pnas.1232342100>
27. Maher AD, Kuchel PW (2003) The Gárdos channel: a review of the Ca^{2+} -activated K^+ channel in human erythrocytes. *Int J Biochem Cell Biol* 35:1182–1197
28. Grygorczyk R (1987) Temperature dependence of Ca^{2+} -activated K^+ currents in the membrane of human erythrocytes. *Biochim Biophys Acta* 902:159–168
29. Rapetti-Mauss R, Lacoste C, Picard V et al (2015) A mutation in the Gardos channel is associated with hereditary xerocytosis. *Blood* 126:1273–1280. <https://doi.org/10.1182/blood-2015-04-642496>
30. Glogowska E, Lezon-Geyda K, Maksimova Y et al (2015) Mutations in the Gardos channel (KCNN4) are associated with hereditary xerocytosis. *Blood* 126:1281–1284. <https://doi.org/10.1182/blood-2015-07-657957>
31. Fermo E, Bogdanova A, Petkova-Kirova P et al (2017) “Gardos Channelopathy”: a variant of hereditary stomatocytosis with complex molecular regulation. *Sci Rep* 7:1744. <https://doi.org/10.1038/s41598-017-01591-w>
32. Mankad VN (2001) Exciting new treatment approaches for pathophysiological mechanisms of sickle cell disease. *Pediatr Pathol Mol Med* 20:1–13

33. Ataga KI, Reid M, Ballas SK et al (2011) Improvements in haemolysis and indicators of erythrocyte survival do not correlate with acute vaso-occlusive crises in patients with sickle cell disease: a phase III randomized, placebo-controlled, double-blind study of the Gardos channel blocker senicapoc (ICA-17043). *Br J Haematol* 153:92–104. <https://doi.org/10.1111/j.1365-2141.2010.08520.x>
34. Bogdanova A, Makhro A, Kaestner L (2015) Calcium handling in red blood cells of sickle cell disease patients. In: Lewis ME (ed) *Sickle cell disease: Genetics, Management and Prognosis*, Nova Publishing, pp 29–59
35. Rapetti-Mauss R, Soriani O, Vinti H et al (2016) Senicapoc: a potent candidate for the treatment of a subset of Hereditary Xerocytosis caused by mutations in the Gardos channel. *Haematologica* 2016:149104. <https://doi.org/10.3324/haematol.2016.149104>
36. Christophersen P, Bennekou P (1991) Evidence for a voltage-gated, non-selective cation channel in the human red cell membrane. *Biochim Biophys Acta* 1065:103–106
37. Bennekou P (1993) The voltage-gated non-selective cation channel from human red cells is sensitive to acetylcholine. *Biochim Biophys Acta* 1147:165–167
38. Kaestner L, Christophersen P, Bernhardt I, Bennekou P (2000) The non-selective voltage-activated cation channel in the human red blood cell membrane: reconciliation between two conflicting reports and further characterisation. *Bioelectrochemistry* 52:117–125
39. Kaestner L (2011) Cation channels in erythrocytes – historical and future perspective. *Open Biol* 4:27–34
40. Bouyer G, Thomas S, Egée S (2012) Patch-clamp analysis of membrane transport in erythrocytes. In: *Patch clamp technique*. InTech, Rijeka, pp 171–202
41. Bouyer G, Cuffe A, Egée S et al (2011) Erythrocyte peripheral type benzodiazepine receptor/voltage-dependent anion channels are upregulated by *Plasmodium falciparum*. *Blood* 118:2305–2312. <https://doi.org/10.1182/blood-2011-01-329300>
42. Moroni M, Servin-Vences MR, Fleischer R et al (2018) Voltage gating of mechanosensitive PIEZO channels. *Nat Commun* 9:1096. <https://doi.org/10.1038/s41467-018-03502-7>
43. Kaestner L, Egée S (2018) Commentary: voltage gating of mechanosensitive PIEZO channels. *Front Physiol* 9:1565
44. Andersson T (2010) Exploring voltage-dependent ion channels in silico by hysteretic conductance. *Math Biosci* 226:16–27. <https://doi.org/10.1016/j.mbs.2010.03.004>
45. Zarychanski R, Schulz VP, Houston BL et al (2012) Mutations in the mechanotransduction protein PIEZO1 are associated with hereditary xerocytosis. *Blood* 120:1908–1915. <https://doi.org/10.1182/blood-2012-04-422253>
46. Bae C, Gnanasambandam R, Nicolai C et al (2013) Xerocytosis is caused by mutations that alter the kinetics of the mechanosensitive channel PIEZO1. *Proc Natl Acad Sci U S A* 110:E1162–E1168. <https://doi.org/10.1073/pnas.1219777110>
47. Kaestner L (2015) Channelizing the red blood cell: molecular biology competes with patch-clamp. *Front Mol Biosci* 2:46. <https://doi.org/10.3389/fmolb.2015.00046>
48. Syeda R, Xu J, Dubin AE et al (2015) Chemical activation of the mechanotransduction channel Piezo1. *Elife*. <https://doi.org/10.7554/eLife.07369>
49. Rotordam GM, Fermo E, Becker N et al (2019) A novel gain-of-function mutation of Piezo1 is functionally affirmed in red blood cells by high-throughput patch clamp. *Haematologica* 104(5). <https://doi.org/10.3324/haematol.2018.201160>
50. Lew VL, Tiffert T (2017) On the mechanism of human red blood cell longevity: roles of calcium, the sodium pump, PIEZO1, and Gardos channels. *Front Physiol* 8:977. <https://doi.org/10.3389/fphys.2017.00977>
51. Albuissou J, Murthy SE, Bandell M et al (2013) Dehydrated hereditary stomatocytosis linked to gain-of-function mutations in mechanically activated PIEZO1 ion channels. *Nat Commun* 4:1884. <https://doi.org/10.1038/ncomms2899>
52. Andolfo I, Alper SL, De Franceschi L et al (2013) Multiple clinical forms of dehydrated hereditary stomatocytosis arise from mutations in PIEZO1. *Blood* 121:3925–3935. <https://doi.org/10.1182/blood-2013-02-482489>
53. Archer NM, Shmukler BE, Andolfo I et al (2014) Hereditary xerocytosis revisited. *Am J Hematol* 89:1142–1146. <https://doi.org/10.1002/ajh.23799>

54. Glogowska E, Schneider ER, Maksimova Y et al (2017) Novel mechanisms of PIEZO1 dysfunction in hereditary xerocytosis. *Blood* 130:1845–1856. <https://doi.org/10.1182/blood-2017-05-786004>
55. Hertz L, Huisjes R, Laudet-Planas E et al (2017) Is increased intracellular calcium in red blood cells a common component in the molecular mechanism causing anemia? *Front Physiol* 8:673. <https://doi.org/10.3389/fphys.2017.00673>
56. Steffen P, Jung A, Nguyen DB et al (2011) Stimulation of human red blood cells leads to Ca^{2+} -mediated intercellular adhesion. *Cell Calcium* 50:54–61. <https://doi.org/10.1016/j.ceca.2011.05.002>
57. Kaestner L, Steffen P, Nguyen DB et al (2012) Lysophosphatidic acid induced red blood cell aggregation in vitro. *Bioelectrochemistry* 87:89–95. <https://doi.org/10.1016/j.bioelechem.2011.08.004>
58. Chung SM, Bae ON, Lim KM et al (2007) Lysophosphatidic acid induces thrombogenic activity through phosphatidylserine exposure and procoagulant microvesicle generation in human erythrocytes. *Arterioscler Thromb Vasc Biol* 27:414–421
59. Lew VL, Ortiz OE, Bookchin RM (1997) Stochastic nature and red cell population distribution of the sickling-induced Ca^{2+} permeability. *J Clin Invest* 99:2727–2735. <https://doi.org/10.1172/JCI119462>
60. Browning JA, Robinson HC, Ellory JC, Gibson JS (2007) Deoxygenation-induced non-electrolyte pathway in red cells from sickle cell patients. *Cell Physiol Biochem* 19:165–174. <https://doi.org/10.1159/000099204>
61. Ma Y-L, Rees DC, Gibson JS, Ellory JC (2012) The conductance of red blood cells from sickle cell patients: ion selectivity and inhibitors. *J Physiol Lond* 590:2095–2105. <https://doi.org/10.1113/jphysiol.2012.229609>
62. Bae C, Sachs F, Gottlieb PA (2011) The mechanosensitive ion channel Piezo1 is inhibited by the peptide GsMTx4. *Biochemistry* 50:6295–6300. <https://doi.org/10.1021/bi200770q>
63. Hanggi P, Makhro A, Gassmann M et al (2014) Red blood cells of sickle cell disease patients exhibit abnormally high abundance of N-methyl D-aspartate receptors mediating excessive calcium uptake. *Br J Haematol* 167:252–264. <https://doi.org/10.1111/bjh.13028>
64. Makhro A, Wang J, Vogel J et al (2010) Functional NMDA receptors in rat erythrocytes. *Am J Physiol Cell Physiol* 298:C1315–C1325. <https://doi.org/10.1152/ajpcell.00407.2009>
65. Bogdanova A, Makhro A, Goede J et al (2009) NMDA receptors in mammalian erythrocytes. *Clin Biochem* 42:1858–1859
66. Makhro A, Kaestner L, Bogdanova A (2017) NMDA receptor activity in circulating red blood cells: methods of detection. *Methods Mol Biol* 1677:265–282, 484. https://doi.org/10.1007/978-1-4939-7321-7_15
67. Hanggi P, Telezhkin V, Kemp PJ et al (2015) Functional plasticity of the N-methyl-d-aspartate receptor in differentiating human erythroid precursor cells. *Am J Physiol Cell Physiol* 308:C993–C1007. <https://doi.org/10.1152/ajpcell.00395.2014>
68. Hegemann I, Sasselli C, Valeri F, Makhro A, Müller R, Bogdanova A, Manz MG, Gassmann M, Goede JS. Memantine treatment is well tolerated by sickle cell patients and improves erythrocyte stability: phase II study MemSID (submitted)
69. Bogdanova A, Makhro A, Hegemann I, Seiler E, Bogdanov N, Simionato G, Kaestner L, Claveria V, Saselli C, Torgeson P, Manz M, Goede J, Gassmann M. Improved maturation and increased stability of red blood cells of sickle cell patients on memantine treatment (submitted)
70. Makhro A, Haider T, Wang J et al (2016) Comparing the impact of an acute exercise bout on plasma amino acid composition, intraerythrocytic Ca^{2+} handling, and red cell function in athletes and untrained subjects. *Cell Calcium* 60:235–244. <https://doi.org/10.1016/j.ceca.2016.05.005>
71. Thomas SLY, Bouyer G, Cuff A et al (2011) Ion channels in human red blood cell membrane: actors or relics? *Blood Cells Mol Dis* 46:261–265. <https://doi.org/10.1016/j.bcmd.2011.02.007>
72. Schein SJ, Colombini M, Finkelstein A (1976) Reconstitution in planar lipid bilayers of a voltage-dependent anion-selective channel obtained from paramecium mitochondria. *J Membr Biol* 30:99–120

73. Thinnies FP, Flörke H, Winkelbach H et al (1994) Channel active mammalian porin, purified from crude membrane fractions of human B lymphocytes or bovine skeletal muscle, reversibly binds the stilbene-disulfonate group of the chloride channel blocker DIDS. *Biol Chem Hoppe Seyler* 375:315–322
74. Marginedas-Freixa I, Hattab C, Bouyer G et al (2016) TSPO ligands stimulate ZnPPIX transport and ROS accumulation leading to the inhibition of *P. falciparum* growth in human blood. *Sci Rep* 6:33516. <https://doi.org/10.1038/srep33516>
75. McEnery MW, Snowman AM, Trifiletti RR, Snyder SH (1992) Isolation of the mitochondrial benzodiazepine receptor: association with the voltage-dependent anion channel and the adenine nucleotide carrier. *Proc Natl Acad Sci U S A* 89:3170–3174
76. Le Fur G, Vaucher N, Perrier ML et al (1983) Differentiation between two ligands for peripheral benzodiazepine binding sites, [3H]RO5-4864 and [3H]PK 11195, by thermodynamic studies. *Life Sci* 33:449–457
77. Olson JM, Ciliax BJ, Mancini WR, Young AB (1988) Presence of peripheral-type benzodiazepine binding sites on human erythrocyte membranes. *Eur J Pharmacol* 152:47–53
78. Canat X, Carayon P, Bouaboula M et al (1993) Distribution profile and properties of peripheral-type benzodiazepine receptors on human hemopoietic cells. *Life Sci* 52:107–118
79. Shoshan-Barmatz V, De Pinto V, Zweckstetter M et al (2010) VDAC, a multi-functional mitochondrial protein regulating cell life and death. *Mol Asp Med* 31:227–285. <https://doi.org/10.1016/j.mam.2010.03.002>
80. Moran O, Sorgato MC (1992) High-conductance pathways in mitochondrial membranes. *J Bioenerg Biomembr* 24:91–98
81. Benz R (1994) Permeation of hydrophilic solutes through mitochondrial outer membranes: review on mitochondrial porins. *Biochim Biophys Acta* 1197:167–196
82. Hodge T, Colombini M (1997) Regulation of metabolite flux through voltage-gating of VDAC channels. *J Membr Biol* 157:271–279
83. Gincel D, Silberberg SD, Shoshan-Barmatz V (2000) Modulation of the voltage-dependent anion channel (VDAC) by glutamate. *J Bioenerg Biomembr* 32:571–583
84. Báthori G, Csordás G, Garcia-Perez C et al (2006) Ca²⁺-dependent control of the permeability properties of the mitochondrial outer membrane and voltage-dependent anion-selective channel (VDAC). *J Biol Chem* 281:17347–17358. <https://doi.org/10.1074/jbc.M600906200>
85. Tong Q, Hirschler-Laszkiwicz I, Zhang W et al (2008) TRPC3 is the erythropoietin-regulated calcium channel in human erythroid cells. *J Biol Chem* 283:10385–10395. <https://doi.org/10.1074/jbc.M710231200>
86. Hirschler-Laszkiwicz I, Tong Q, Conrad K et al (2009) TRPC3 activation by erythropoietin is modulated by TRPC6. *J Biol Chem* 284:4567–4581. <https://doi.org/10.1074/jbc.M804734200>
87. Kucherenko YV, Bhavsar SK, Grischenko VI et al (2010) Increased cation conductance in human erythrocytes artificially aged by glycation. *J Membr Biol* 235:177–189. <https://doi.org/10.1007/s00232-010-9265-2>
88. Danielczok J, Hertz L, Ruppenthal S et al (2017) Does erythropoietin regulate TRPC channels in red blood cells? *Cell Physiol Biochem* 41:1219–1228. <https://doi.org/10.1159/000464384>
89. Foller M, Kasinathan RS, Koka S et al (2008) TRPC6 contributes to the Ca²⁺ leak of human erythrocytes. *Cell Physiol Biochem* 21:183–192
90. Dietrich A, Gudermann T (2014) TRPC6: physiological function and pathophysiological relevance. *Handb Exp Pharmacol* 222:157–188. https://doi.org/10.1007/978-3-642-54215-2_7
91. Pinet C, Antoine S, Filoteo AG et al (2002) Reincorporated plasma membrane Ca²⁺-ATPase can mediate B-type Ca²⁺ channels observed in native membrane of human red blood cells. *J Membr Biol* 187:185–201. <https://doi.org/10.1007/s00232-001-0163-5>
92. Romero PJ, Romero EA, Mateu D et al (2006) Voltage-dependent calcium channels in young and old human red cells. *Cell Biochem Biophys* 46:265–276. <https://doi.org/10.1385/CBB:46:3:265>
93. Andrews DA, Yang L, Low PS (2002) Phorbol ester stimulates a protein kinase C-mediated agatoxin-TK-sensitive calcium permeability pathway in human red blood cells. *Blood* 100:3392–3399

94. Wagner-Britz L, Wang J, Kaestner L, Bernhardt I (2013) Protein kinase C α and P-type Ca channel CaV2.1 in red blood cell calcium signalling. *Cell Physiol Biochem* 31:883–891. <https://doi.org/10.1159/000350106>
95. Kaestner L, Wang X, Hertz L, Bernhardt I (2018) Voltage-activated ion channels in non-excitable cells – a viewpoint regarding their physiological justification. *Front Physiol* 9:450
96. Tiffert T, Bookchin RM, Lew VL (2003) Calcium homeostasis in normal and abnormal human red cells. In: Bernhardt I, Ellory C (eds) *Red cell membrane transport in health and disease*. Springer, Berlin, pp 373–405
97. Catterall WA (2011) Voltage-gated calcium channels. *Cold Spring Harb Perspect Biol* 3:a003947. <https://doi.org/10.1101/cshperspect.a003947>
98. Catterall WA (2000) Structure and regulation of voltage-gated Ca $^{2+}$ channels. *Annu Rev Cell Dev Biol* 16:521–555. <https://doi.org/10.1146/annurev.cellbio.16.1.521>
99. Petkova-Kirova P, Hertz L, Makhro A et al (2018) A previously unrecognized Ca $^{2+}$ -inhibited non-selective cation channel in red blood cells. *HemaSphere*, 2:e146
100. Flatt JF, Bawazir WM, Bruce LJ (2014) The involvement of cation leaks in the storage lesion of red blood cells. *Front Physiol* 5:214. <https://doi.org/10.3389/fphys.2014.00214>
101. Lipp P, Kaestner L (2014) Detecting calcium in cardiac muscle: fluorescence to dye for. *Am J Physiol Heart Circ Physiol* 307:H1687–H1690. <https://doi.org/10.1152/ajpheart.00468.2014>
102. Kaestner L, Tabellion W, Weiss E et al (2006) Calcium imaging of individual erythrocytes: problems and approaches. *Cell Calcium* 39:13–19. <https://doi.org/10.1016/j.ceca.2005.09.004>
103. Jarrett HW, Kyte J (1979) Human erythrocyte calmodulin. Further chemical characterization and the site of its interaction with the membrane. *J Biol Chem* 254:8237–8244
104. Leinders T, van Kleef RG, Vijverberg HP (1992) Single Ca $^{2+}$ -activated K $^{+}$ channels in human erythrocytes: Ca $^{2+}$ dependence of opening frequency but not of open lifetimes. *Biochim Biophys Acta* 1112:67–74
105. Stout JG, Zhou Q, Wiedmer T, Sims PJ (1998) Change in conformation of plasma membrane phospholipid scramblase induced by occupancy of its Ca $^{2+}$ binding site. *Biochemistry* 37:14860–14866. <https://doi.org/10.1021/bi9812930>
106. Woon LA, Holland JW, Kable EP, Roufogalis BD (1999) Ca $^{2+}$ sensitivity of phospholipid scrambling in human red cell ghosts. *Cell Calcium* 25:313–320
107. Bitbol M, Fellmann P, Zachowski A, Devaux PF (1987) Ion regulation of phosphatidylserine and phosphatidylethanolamine outside-inside translocation in human erythrocytes. *Biochim Biophys Acta* 904:268–282
108. Murakami T, Hatanaka M, Murachi T (1981) The cytosol of human erythrocytes contains a highly Ca $^{2+}$ -sensitive thiol protease (calpain I) and its specific inhibitor protein (calpastatin). *J Biochem* 90:1809–1816
109. Salamino F, De Tullio R, Mengotti P et al (1993) Site-directed activation of calpain is promoted by a membrane-associated natural activator protein. *Biochem J* 290(Pt 1):191–197
110. Bergamini CM, Signorini M (1993) Studies on tissue transglutaminases: interaction of erythrocyte type-2 transglutaminase with GTP. *Biochem J* 291(Pt 1):37–39
111. Almaraz L, García-Sancho J, Lew VL (1988) Calcium-induced conversion of adenine nucleotides to inosine monophosphate in human red cells. *J Physiol Lond* 407:557–567
112. Kohout SC, Corbalán-García S, Torrecillas A et al (2002) C2 domains of protein kinase C isoforms alpha, beta, and gamma: activation parameters and calcium stoichiometries of the membrane-bound state. *Biochemistry* 41:11411–11424. <https://doi.org/10.1021/bi026401k>
113. Schwarz W, Grygorczyk R, Hof D (1989) Recording single-channel currents from human red cells. *Methods Enzymol* 173:112–121
114. Grygorczyk R, Schwarz W, Passow H (1984) Ca $^{2+}$ -activated K $^{+}$ channels in human red cells. Comparison of single-channel currents with ion fluxes. *Biophys J* 45:693–698. [https://doi.org/10.1016/S0006-3495\(84\)84211-3](https://doi.org/10.1016/S0006-3495(84)84211-3)
115. Grygorczyk R, Schwarz W (1985) Ca $^{2+}$ -activated K $^{+}$ permeability in human erythrocytes: modulation of single-channel events. *Eur Biophys J* 12:57–65

116. Leinders T, van Kleef RG, Vijverberg HP (1992) Distinct metal ion binding sites on Ca^{2+} -activated K^+ channels in inside-out patches of human erythrocytes. *Biochim Biophys Acta* 1112:75–82
117. Dunn PM (1998) The action of blocking agents applied to the inner face of Ca^{2+} -activated K^+ channels from human erythrocytes. *J Membr Biol* 165:133–143
118. Wolff D, Cecchi X, Spalvins A, Canessa M (1988) Charybdotoxin blocks with high affinity the Ca -activated K^+ channel of Hb A and Hb S red cells: individual differences in the number of channels. *J Membr Biol* 106:243–252
119. Qadri SM, Kucherenko Y, Lang F (2011) Beauvericin induced erythrocyte cell membrane scrambling. *Toxicology* 283:24–31. <https://doi.org/10.1016/j.tox.2011.01.023>
120. Kucherenko Y, Zelenak C, Eberhard M et al (2012) Effect of casein kinase 1 α activator pyrvinium pamoate on erythrocyte ion channels. *Cell Physiol Biochem* 30:407–417. <https://doi.org/10.1159/000339034>
121. Kucherenko YV, Wagner-Britz L, Bernhardt I, Lang F (2013) Effect of chloride channel inhibitors on cytosolic Ca^{2+} levels and Ca^{2+} -activated K^+ (Gardos) channel activity in human red blood cells. *J Membr Biol* 246:315–326. <https://doi.org/10.1007/s00232-013-9532-0>
122. Baunbaek M, Bennekou P (2008) Evidence for a random entry of Ca^{2+} into human red cells. *Bioelectrochemistry* 73:145–150. <https://doi.org/10.1016/j.bioelechem.2008.04.006>
123. Seear RV, Lew VL (2011) IKCa agonist (NS309)-elicited all-or-none dehydration response of human red blood cells is cell-age dependent. *Cell Calcium* 50:444–448. <https://doi.org/10.1016/j.ceca.2011.07.005>
124. Schatzmann HJ (1973) Dependence on calcium concentration and stoichiometry of the calcium pump in human red cells. *J Physiol Lond* 235:551–569
125. Lines GT, Sande JB, Louch WE et al (2006) Contribution of the $\text{Na}^+/\text{Ca}^{2+}$ exchanger to rapid Ca^{2+} release in cardiomyocytes. *Biophys J* 91:779–792. <https://doi.org/10.1529/biophysj.105.072447>
126. Chu H, Puchulu-Campanella E, Galan JA et al (2012) Identification of cytoskeletal elements enclosing the ATP pools that fuel human red blood cell membrane cation pumps. *Proc Natl Acad Sci U S A* 109:12794–12799. <https://doi.org/10.1073/pnas.1209014109>
127. Bers DM (2002) Cardiac excitation-contraction coupling. *Nature* 415:198–205. <https://doi.org/10.1038/415198a>
128. Rasband MN, Shrager P (2000) Ion channel sequestration in central nervous system axons. *J Physiol Lond* 525(Pt 1):63–73. <https://doi.org/10.1111/j.1469-7793.2000.00063.x>
129. Dyrda A, Cytlak U, Ciuraszkiwicz A et al (2010) Local membrane deformations activate Ca^{2+} -dependent K^+ and anionic currents in intact human red blood cells. *PLoS One* 5:e9447. <https://doi.org/10.1371/journal.pone.0009447>
130. Liappis N (1972) Sodium-, potassium- and chloride-concentrations in the serum of infants, children and adults. *Monatsschr Kinderheilkd* 120:138–142